



FACULTY OF ENGINEERING
ALEXANDRIA UNIVERSITY

Alexandria University
Alexandria Engineering Journal

www.elsevier.com/locate/aej
www.sciencedirect.com



ORIGINAL ARTICLE

Peristaltic transport of a Carreau fluid in a compliant rectangular duct



Arshad Riaz ^{a,*}, R. Ellahi ^a, S. Nadeem ^b

^a Department of Mathematics and Statistics, FBAS, IIU, Islamabad 44000, Pakistan

^b Department of Mathematics, Quaid-i-Azam University, 45320, Islamabad 44000, Pakistan

Received 5 September 2013; revised 9 January 2014; accepted 16 January 2014

Available online 14 February 2014

KEYWORDS

Peristaltic flow;
Carreau fluid;
Rectangular duct;
Compliant walls;
Analytical solution

Abstract The study of peristaltic flow of a Carreau fluid in a compliant rectangular channel has been analyzed in this article. The assumptions of low Reynolds number and long wavelength approximation are utilized here to simplify the complicated governing equations for the three dimensional flow geometry. The resulting highly non-linear partial differential constitutive equations are solved jointly by homotopy perturbation and Eigen function expansion methods. The effects of various physical parameters on velocity distribution have been observed graphically for both two and three dimensional aspects. The trapping scheme has also been discussed by plotting stream lines.

© 2014 Production and hosting by Elsevier B.V. on behalf of Faculty of Engineering, Alexandria University.

1. Introduction

The study of peristaltic flows plays a vital role in physiology and industry because of its large number of applications and in mathematics for its complicated geometries and non-linear problems. In physiology, it is applied by many systems in the living body to propel or to mix the contents of a tube. The

peristaltic mechanism usually follows in urine transport from kidney to bladder, swallowing food through esophagus, chyme motion in the gastrointestinal tracts, vasomotion of small blood vessels, movement of Spermatozoa and the human reproductive tract. Theoretically and mathematically, the complete exact solutions of peristaltic flow problems are quite complex to evaluate even in viscous fluid theory. However, by applying certain physical simplifications such as long wavelength and low Reynolds number approximations, the authors successfully calculate only limited exact and analytical solutions. The study of peristaltic flows of non-Newtonian fluids has achieved considerable attention in the past few years. There are several investigations to study the different aspects of peristaltic flows with different flow geometries. Mention may be made to the interesting works of [1–14]. Recently, Abd Elnaby and Haroun [15] have presented a new model for study the effect of wall properties on peristaltic

* Corresponding author. Tel.: +92 05190642182.

E-mail address: arshad.phdma03@iiu.edu.pk (A. Riaz).

Peer review under responsibility of Faculty of Engineering, Alexandria University.



Production and hosting by Elsevier

transport of viscous fluid. Basically the study of compliant wall is useful for controlling the muscles tension. The action of these muscles has been discussed mathematically by a set of equations which are related to compliant wall displacement [16,17]. Srinivasvas and Kothandapani [18] have examined the combined effects of heat and mass transfer on MHD peristaltic flow through a porous space with compliant walls. However, all the studies are discussed for two dimensional channels. In peristaltic problems only a limited attention has been given to the study of three dimensional channels or in a rectangular channel [11–14,19–21]. However, the peristaltic flow of Newtonian or non-Newtonian fluid in a rectangular channel with compliant walls is not discussed so far. Due to a large number of applications of peristaltic phenomenon in industry, clinical equipment and engineering, the researchers and developers are keen to concentrate on the peristaltic flows of non-Newtonian fluids in three dimensional channels. Motivated from the above recent development in the field of peristalsis, this study is presented to evaluate the peristaltic flow of Carreau fluid in a rectangular channel having flexible walls. The governing equations of a Carreau fluid are simplified by using assumption of low Reynolds number and long wavelength approximation. The reduced equations are finally solved analytically by homotopy perturbation and Eigen function expansion methods. The physical features of all the related parameters have been highlighted through graphs. The trapping phenomenon is also discussed at the end of the paper.

2. Mathematical formulation

Let us take the peristaltic transport of an incompressible Carreau fluid in a cross section of rectangular duct having the channel width $2d$ and height $2a$. The Cartesian coordinate system is being taken for the geometry [19]. The walls of the channel have the property of being compliant. The flow is assumed to be produced by the sinusoidal waves having long wavelength λ . The peristaltic waves on the walls are described as

$$z = h(x, t) = \pm a \pm b \cos \left[\frac{2\pi}{\lambda} (x - ct) \right],$$

where a and b are the amplitudes of the waves, c is the velocity of the propagation, t is the time and x is the direction of wave propagation. We assume that the lateral velocity is zero as there is no change in lateral direction (y -axis). Let $(u, 0, w)$ be the velocity for a mentioned geometry. The governing equations for the flow under observation are stated as

$$\frac{\partial u}{\partial x} + \frac{\partial w}{\partial z} = 0, \quad (1)$$

$$\rho \left(\frac{\partial u}{\partial t} + u \frac{\partial u}{\partial x} + w \frac{\partial u}{\partial z} \right) = -\frac{\partial p}{\partial x} + \frac{\partial}{\partial x} S_{xx} + \frac{\partial}{\partial y} S_{xy} + \frac{\partial}{\partial z} S_{xz}, \quad (2)$$

$$0 = -\frac{\partial p}{\partial y} + \frac{\partial}{\partial x} S_{yx} + \frac{\partial}{\partial y} S_{yy} + \frac{\partial}{\partial z} S_{yz}, \quad (3)$$

$$\rho \left(\frac{\partial w}{\partial t} + u \frac{\partial w}{\partial x} + w \frac{\partial w}{\partial z} \right) = -\frac{\partial p}{\partial z} + \frac{\partial}{\partial x} S_{zx} + \frac{\partial}{\partial y} S_{zy} + \frac{\partial}{\partial z} S_{zz}, \quad (4)$$

in which ρ is the density, p is the pressure and \mathbf{S} is the stress tensor for Carreau fluid, which is defined as [11]

$$\mathbf{S} = \mu \left(1 + (\Gamma \dot{\gamma})^2 \right)^{\frac{n-1}{2}} \dot{\gamma}. \quad (5)$$

Defining the following non-dimensional quantities

$$\begin{aligned} \bar{x} &= \frac{x}{\lambda}, & \bar{y} &= \frac{y}{d}, & \bar{z} &= \frac{z}{a}, & \bar{u} &= \frac{u}{c}, & \bar{w} &= \frac{w}{c\delta}, & \bar{t} &= \frac{ct}{\lambda}, \\ \bar{h} &= \frac{h}{a}, & \bar{p} &= \frac{a^2 p}{\mu c \lambda}, & \bar{\gamma} &= \frac{d}{c} \dot{\gamma}, & Re &= \frac{\rho a c}{\mu}, & \delta &= \frac{a}{\lambda}, \\ \phi &= \frac{b}{a}, & \beta &= \frac{a}{d}, & We &= \frac{\Gamma c}{d}, & \bar{S}_{xx} &= \frac{a}{\mu c} S_{xx}, & \bar{S}_{xy} &= \frac{d}{\mu c} S_{xy}, \\ \bar{S}_{yz} &= \frac{d}{\mu c} S_{yz}, & \bar{S}_{zz} &= \frac{\lambda}{\mu c} S_{zz}, & \bar{S}_{yy} &= \frac{\lambda}{\mu c} S_{yy}, & \bar{S}_{xz} &= \frac{a}{\mu c} S_{xz}. \end{aligned}$$

Using the above non-dimensional quantities in Eqs. (1)–(4), the resulting equations after dropping the bars can be written as

$$\frac{\partial u}{\partial x} + \frac{\partial w}{\partial z} = 0, \quad (6)$$

$$Re \delta \left(\frac{\partial u}{\partial t} + u \frac{\partial u}{\partial x} + w \frac{\partial u}{\partial z} \right) = -\frac{\partial p}{\partial x} + \delta \frac{\partial}{\partial x} S_{xx} + \beta^2 \frac{\partial}{\partial y} S_{xy} + \frac{\partial}{\partial z} S_{xz}, \quad (7)$$

$$0 = -\frac{\partial p}{\partial y} + \delta^2 \frac{\partial}{\partial x} S_{yx} + \delta^2 \frac{\partial}{\partial y} S_{yy} + \delta \frac{\partial}{\partial z} S_{yz}, \quad (8)$$

$$Re \delta^2 \left(\frac{\partial w}{\partial t} + u \frac{\partial w}{\partial x} + w \frac{\partial w}{\partial z} \right) = -\frac{\partial p}{\partial z} + \delta^2 \frac{\partial}{\partial x} S_{zx} + \delta \beta^2 \frac{\partial}{\partial y} S_{zy} + \delta^2 \frac{\partial}{\partial z} S_{zz}, \quad (9)$$

where

$$S_{xx} = 2\delta \left(1 + \frac{n-1}{2} We^2 \dot{\gamma}^2 \right) \frac{\partial u}{\partial x},$$

$$S_{xy} = \left(1 + \frac{n-1}{2} We^2 \dot{\gamma}^2 \right) \frac{\partial u}{\partial y},$$

$$S_{xz} = \left(1 + \frac{n-1}{2} We^2 \dot{\gamma}^2 \right) \left(\frac{\partial u}{\partial z} + \delta^2 \frac{\partial w}{\partial x} \right),$$

$$S_{yy} = 0,$$

$$S_{yz} = \delta \left(1 + \frac{n-1}{2} We^2 \dot{\gamma}^2 \right) \frac{\partial w}{\partial y},$$

$$S_{zz} = 2 \left(1 + \frac{n-1}{2} We^2 \dot{\gamma}^2 \right) \frac{\partial w}{\partial z},$$

and

$$\begin{aligned} \dot{\gamma}^2 &= 2\delta^2 \left(\frac{\partial u}{\partial x} \right)^2 + \beta^2 \left(\frac{\partial u}{\partial y} \right)^2 + \delta^2 \beta^2 \left(\frac{\partial w}{\partial y} \right)^2 + \delta^2 \left(\frac{\partial w}{\partial z} \right)^2 \\ &+ \left(\delta^2 \frac{\partial w}{\partial x} + \frac{\partial u}{\partial z} \right)^2. \end{aligned}$$

Under the limitations of long wave length $\delta \leq 1$ and low Reynolds number $Re \rightarrow 0$, Eqs. (7)–(9) take the form

$$\begin{aligned} \frac{\partial p}{\partial x} &= \beta^2 \frac{\partial^2 u}{\partial y^2} + \frac{\partial^2 u}{\partial z^2} + \frac{n-1}{2} We^2 \beta^4 \frac{\partial}{\partial y} \left(\frac{\partial u}{\partial y} \right)^3 \\ &+ \frac{n-1}{2} We^2 \frac{\partial}{\partial z} \left(\frac{\partial u}{\partial z} \right)^3 + \frac{n-1}{2} We^2 \beta^2 \frac{\partial}{\partial y} \left(\frac{\partial u}{\partial y} \left(\frac{\partial u}{\partial z} \right)^2 \right) \\ &+ \frac{n-1}{2} We^2 \beta^2 \frac{\partial}{\partial z} \left(\frac{\partial u}{\partial z} \left(\frac{\partial u}{\partial y} \right)^2 \right), \end{aligned} \quad (10)$$

$$\frac{\partial p}{\partial y} = 0, \tag{11}$$

$$\frac{\partial p}{\partial z} = 0. \tag{12}$$

From above equation, it is observed that p is not a function of z . Now from Eq. (10), we obtain

$$\begin{aligned} &\beta^2 \frac{\partial^3 u}{\partial z \partial y^2} + \frac{\partial^3 u}{\partial z^3} + \frac{n-1}{2} We^2 \beta^4 \frac{\partial}{\partial z} \left(\frac{\partial}{\partial y} \left(\frac{\partial u}{\partial y} \right)^3 \right) \\ &+ \frac{n-1}{2} We^2 \frac{\partial^2}{\partial z^2} \left(\frac{\partial u}{\partial z} \right)^3 + \frac{n-1}{2} We^2 \beta^2 \frac{\partial^2}{\partial y \partial z} \left(\frac{\partial u}{\partial y} \left(\frac{\partial u}{\partial z} \right)^2 \right) \\ &+ \frac{n-1}{2} We^2 \beta^2 \frac{\partial^2}{\partial z^2} \left(\frac{\partial u}{\partial z} \left(\frac{\partial u}{\partial y} \right)^2 \right) = 0. \end{aligned} \tag{13}$$

The corresponding boundary conditions (in non-dimensional form) for rectangular duct are given as

$$u = -1 \text{ at } y = \pm 1 \text{ and } u = -1 \text{ at } z = \pm 1 \pm \eta(x, t). \tag{14}$$

The governing equation for the flexible walls [21] may be described as

$$L(\eta) = p - p_0, \tag{15}$$

where $\eta(x, t) = \phi \cos 2\pi(x - t)$ and L is an operator, which is used to represent the motion of stretched membrane with viscosity damping forces such that

$$L = m \frac{\partial^2}{\partial t^2} + D \frac{\partial}{\partial t} + B \frac{\partial^4}{\partial x^4} - T \frac{\partial^2}{\partial x^2} + K. \tag{16}$$

In the above equation, m is the mass per unit area, D is the coefficient of the viscous damping forces, B is the flexural rigidity of the plate, T is the elastic tension per unit width in the membrane, K is spring stiffness and p_0 is the pressure on the outside surface of the wall due to tension in the muscle, which is assumed to be zero here. The continuity of stress at $z = \pm 1 \pm \eta$ and using Eq. (10), yield

$$\begin{aligned} \frac{\partial L(\eta)}{\partial x} &= \frac{\partial}{\partial x} \left(E_1 \frac{\partial^2 \eta}{\partial t^2} + E_2 \frac{\partial \eta}{\partial t} + E_3 \frac{\partial^4 \eta}{\partial x^4} - E_4 \frac{\partial^2 \eta}{\partial x^2} + E_5 \eta \right) \\ &= \frac{\partial p}{\partial x}, \end{aligned} \tag{17}$$

$$\begin{aligned} &\frac{\partial}{\partial x} \left(E_1 \frac{\partial^2 \eta}{\partial t^2} + E_2 \frac{\partial \eta}{\partial t} + E_3 \frac{\partial^4 \eta}{\partial x^4} - E_4 \frac{\partial^2 \eta}{\partial x^2} + E_5 \eta \right) \\ &= \beta^2 \frac{\partial^2 u}{\partial y^2} + \frac{\partial^2 u}{\partial z^2} + \frac{n-1}{2} We^2 \beta^4 \frac{\partial}{\partial y} \left(\frac{\partial u}{\partial y} \right)^3 + \frac{n-1}{2} We^2 \\ &\quad \times \frac{\partial}{\partial z} \left(\frac{\partial u}{\partial z} \right)^3 + \frac{n-1}{2} We^2 \beta^2 \frac{\partial}{\partial y} \left(\frac{\partial u}{\partial y} \left(\frac{\partial u}{\partial z} \right)^2 \right) \\ &\quad + \frac{n-1}{2} We^2 \beta^2 \frac{\partial}{\partial z} \left(\frac{\partial u}{\partial z} \left(\frac{\partial u}{\partial y} \right)^2 \right) \text{ at } z \\ &= \pm 1 \pm \eta(x, t), \end{aligned} \tag{18}$$

where $E_1 = ma^3c/\lambda^3\mu$, $E_2 = Da^3/\mu\lambda^2$, $E_3 = Ba^3/c\mu\lambda^5$, $sE_4 = Ta^3/c\mu\lambda^3$ and $E_5 = Ka^3/c\mu\lambda$ are the non-dimensional elasticity parameters.

3. Solution of the problem

Eq. (13) can be integrated to reduce the order of the partial differential equation as follows

$$\begin{aligned} &\beta^2 \frac{\partial^2 u}{\partial y^2} + \frac{\partial^2 u}{\partial z^2} + \frac{n-1}{2} We^2 \beta^4 \frac{\partial}{\partial y} \left(\frac{\partial u}{\partial y} \right)^3 + \frac{n-1}{2} We^2 \frac{\partial}{\partial z} \left(\frac{\partial u}{\partial z} \right)^3 \\ &+ \frac{n-1}{2} We^2 \beta^2 \frac{\partial}{\partial y} \left(\frac{\partial u}{\partial y} \left(\frac{\partial u}{\partial z} \right)^2 \right) \\ &+ \frac{n-1}{2} We^2 \beta^2 \frac{\partial}{\partial z} \left(\frac{\partial u}{\partial z} \left(\frac{\partial u}{\partial y} \right)^2 \right) = D, \end{aligned} \tag{19}$$

where D is a constant of integration to be evaluated. The solution of the above non-linear and non-homogeneous partial differential equation with boundary conditions (14) and (18) has been calculated by using Homotopy perturbation method (HPM), which is defined as [22,23]

$$\begin{aligned} H(v, q) &= L(v) - L(u_0) + qL(u_0) + q \left(\frac{n-1}{2} We^2 \beta^4 \frac{\partial}{\partial y} \left(\frac{\partial v}{\partial y} \right)^3 \right. \\ &+ \frac{n-1}{2} We^2 \frac{\partial}{\partial z} \left(\frac{\partial v}{\partial z} \right)^3 + \frac{n-1}{2} We^2 \beta^2 \frac{\partial}{\partial y} \left(\frac{\partial v}{\partial y} \left(\frac{\partial v}{\partial z} \right)^2 \right) \\ &\left. + \frac{n-1}{2} We^2 \beta^2 \frac{\partial}{\partial z} \left(\frac{\partial v}{\partial z} \left(\frac{\partial v}{\partial y} \right)^2 \right) - D \right), \end{aligned} \tag{20}$$

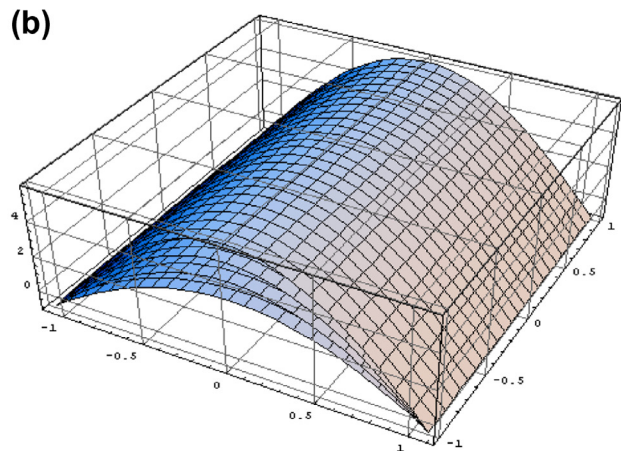
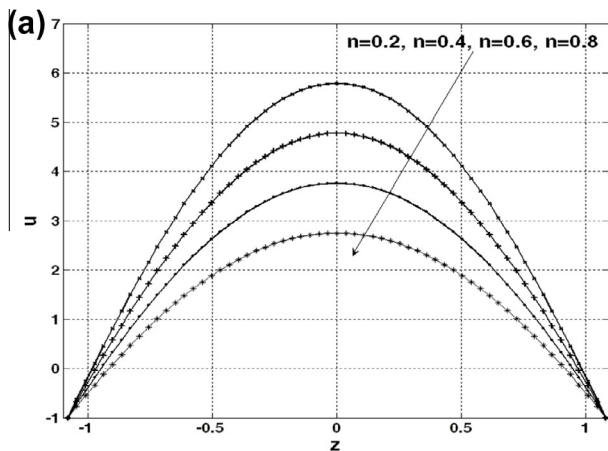


Figure 1 Velocity profile for different values of n for fixed $y = 1$, $\beta = 1.5$, $We = 0.9$, $\phi = 0.1$, $x = 0.5$, $t = 0.4$, $E_1 = 0.1$, $E_2 = 0.2$, $E_3 = 0.01$, $E_4 = 0.2$, $E_5 = 0.3$. (a) For 2-dimensional and (b) for 3-dimensional.

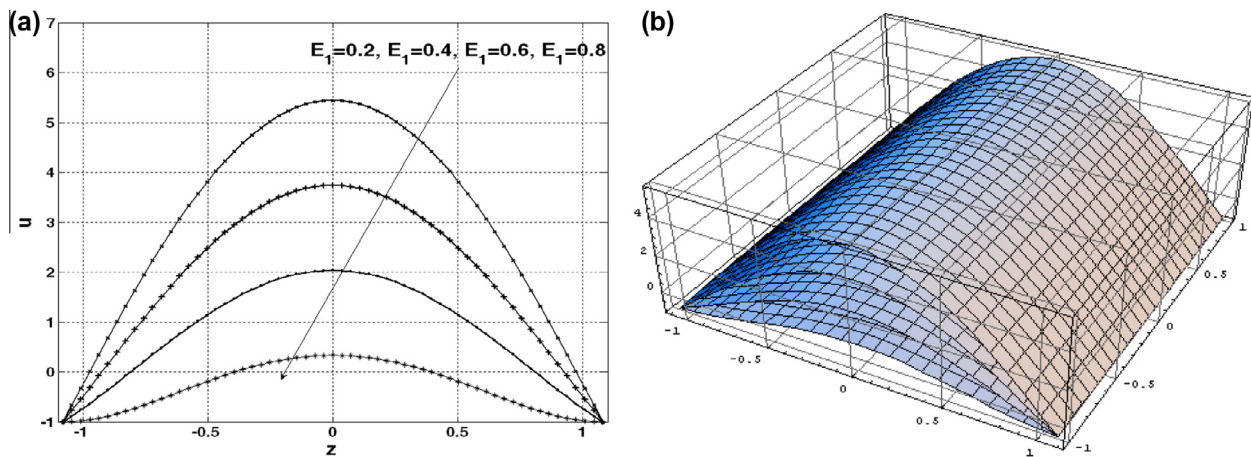


Figure 2 Velocity profile for different values of E_1 for fixed $y = 1, n = 0.1, We = 0.9, \phi = 0.1, x = 0.5, t = 0.4, \beta = 1.5, E_2 = 0.2, E_3 = 0.01, E_4 = 0.2, E_5 = 0.3$. (a) For 2-dimensional and (b) for 3-dimensional.

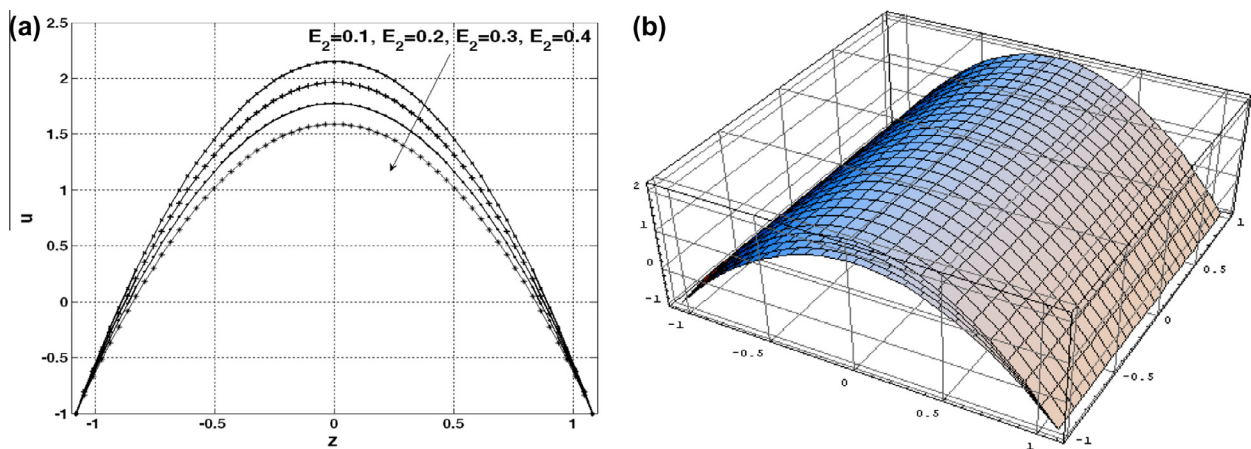


Figure 3 Velocity profile for different values of E_2 for fixed $y = 1, n = 0.1, We = 0.2, \phi = 0.1, x = 0.5, t = 0.4, E_1 = 0.1, \beta = 1.5, E_3 = 0.01, E_4 = 0.2, E_5 = 0.3$. (a) For 2-dimensional and (b) for 3-dimensional.

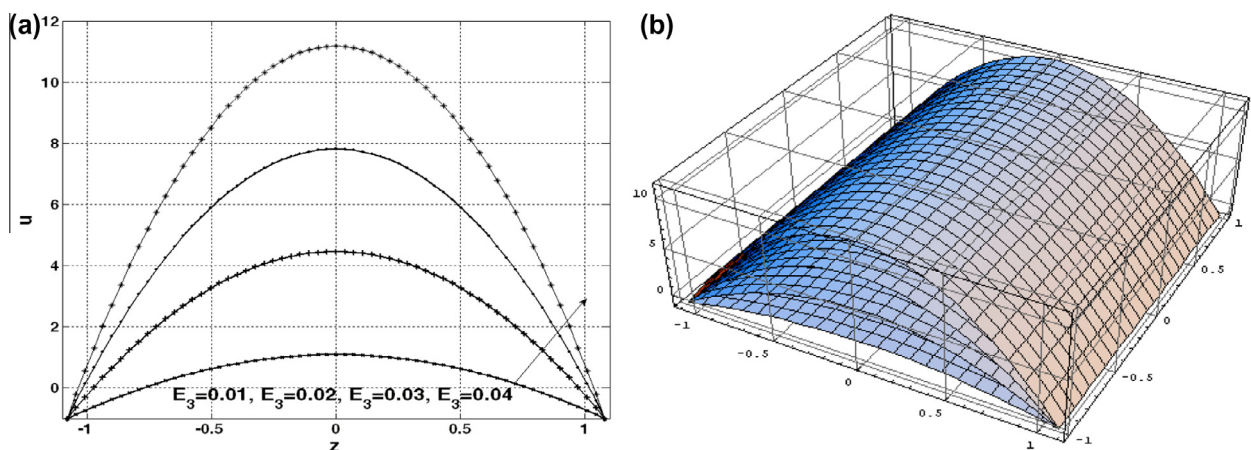


Figure 4 Velocity profile for different values of E_3 for fixed $y = 1, n = 0.1, We = 0.2, \phi = 0.1, x = 0.5, t = 0.4, E_1 = 0.2, E_2 = 0.1, \beta = 0.5, E_4 = 0.1, E_5 = 0.3$. (a) For 2-dimensional and (b) for 3-dimensional.

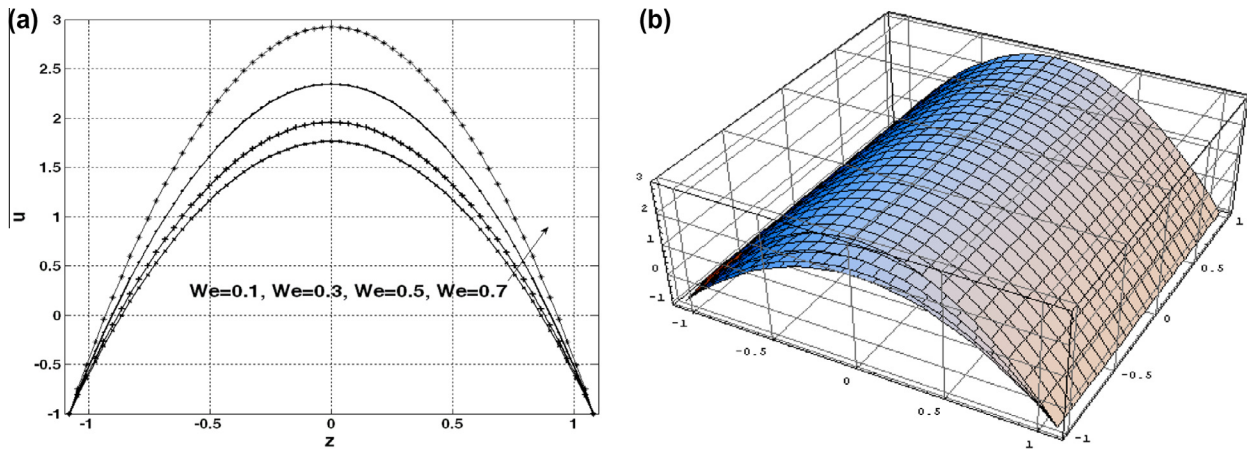


Figure 5 Velocity profile for different values of We for fixed $y = 1$, $n = 0.9$, $\beta = 0.5$, $\phi = 0.1$, $x = 0.5$, $t = 0.4$, $E_1 = 0.1$, $E_2 = 0.2$, $E_3 = 0.01$, $E_4 = 0.2$, $E_5 = 0.3$. (a) For 2-dimensional and (b) for 3-dimensional.

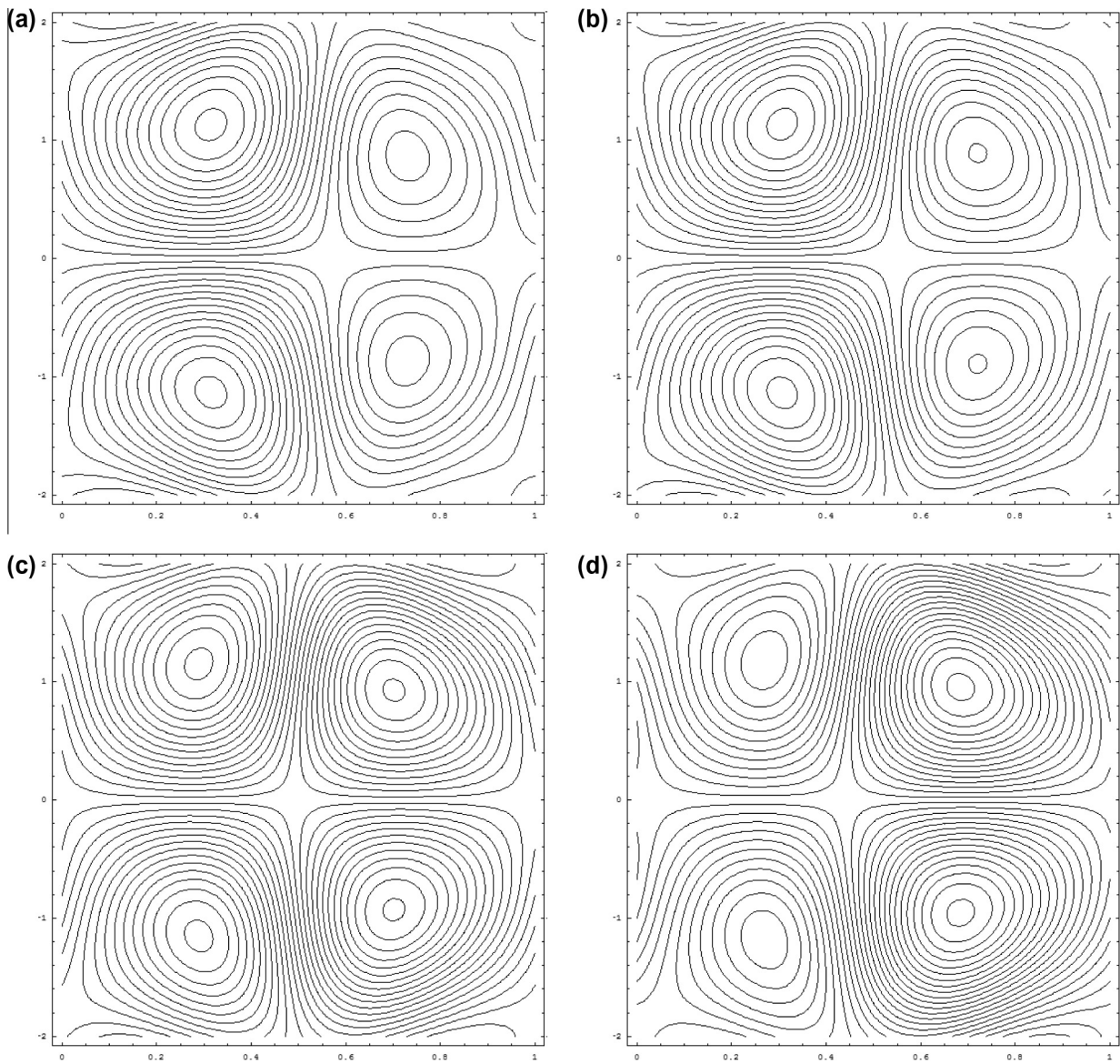


Figure 6 Stream lines for different values of We . (a) For $We = 0.1$, (b) for $We = 0.4$, (c) for $We = 0.7$, (d) for $We = 0.9$. The other parameters are $y = 1$, $\phi = 0.1$, $t = 0.5$, $n = 0.1$, $\beta = 1.5$, $E_1 = 0.2$, $E_2 = 0.2$, $E_3 = 0.01$, $E_4 = 0.2$, $E_5 = 0.3$.

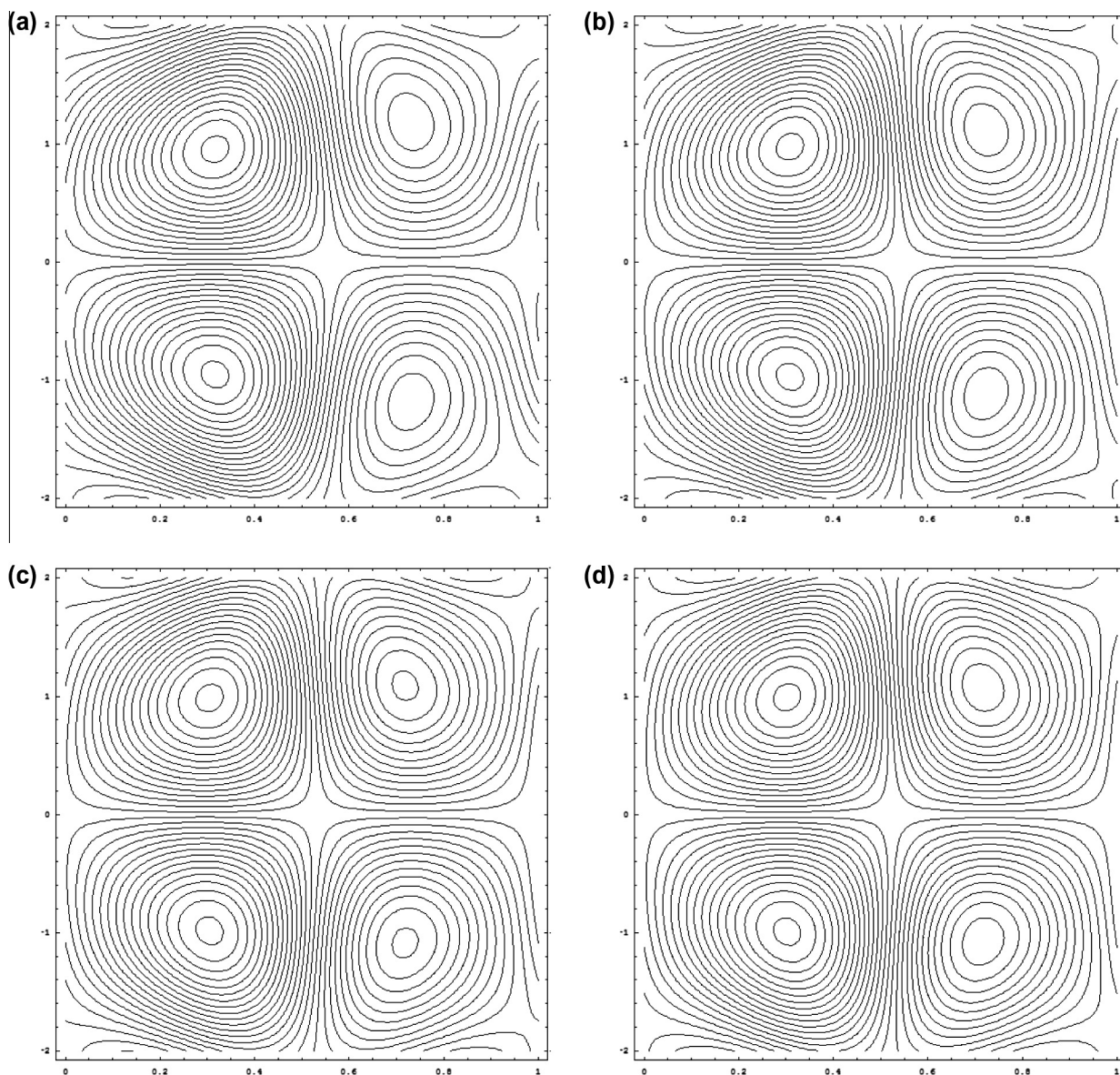


Figure 7 Stream lines for different values of E_1 . (a) For $E_1 = 1$, (b) for $E_1 = 1.2$, (c) for $E_1 = 1.4$, (d) for $E_1 = 1.6$. The other parameters are $y = 1, \phi = 0.1, t = 0.5, n = 0.1, We = 0.9, \beta = 1.5, E_2 = 0.2, E_3 = 0.01, E_4 = 0.2, E_5 = 0.3$.

in which q is embedding parameter which has the range $0 \leq q \leq 1$. For our convenience, we have assumed $L = \beta^2 \frac{\partial^2}{\partial y^2} + \frac{\partial^2}{\partial z^2}$ as the linear operator. The initial guess for the selected operator is chosen as

$$u_0 = -1 + z^2 - h^2 + \frac{1}{\beta^2}(1 - y^2). \tag{21}$$

According to the perturbation technique, let us define

$$v = v_0 + qv_1 + q^2v_2 + \dots \tag{22}$$

Substituting Eq. (22) into Eq. (20) and then comparing the like powers of q , one obtains the following problems with the corresponding boundary conditions

$$L(v_0) - L(u_0) = 0, \tag{23}$$

$$v_0 = -1 \text{ at } y = \pm 1, \tag{24}$$

$$v_0 = -1 \text{ at } z = \pm 1 \pm \eta(x, t), \tag{25}$$

$$\begin{aligned} L(v_1) + L(u_0) + \left(\frac{n-1}{2} We^2 \beta^4 \frac{\partial}{\partial y} \left(\frac{\partial v_0}{\partial y}\right)^3 \right. \\ \left. + \frac{n-1}{2} We^2 \frac{\partial}{\partial z} \left(\frac{\partial v_0}{\partial z}\right)^3 + \frac{n-1}{2} We^2 \beta^2 \frac{\partial}{\partial y} \left(\frac{\partial v_0}{\partial y} \left(\frac{\partial v_0}{\partial z}\right)^2\right) \right. \\ \left. + \frac{n-1}{2} We^2 \beta^2 \frac{\partial}{\partial z} \left(\frac{\partial v_0}{\partial z} \left(\frac{\partial v_0}{\partial y}\right)^2\right) - D \right) = 0, \end{aligned} \tag{26}$$

$$v_1 = 0 \text{ at } y = \pm 1, \tag{27}$$

$$v_1 = 0, \text{ at } z = \pm 1 \pm \eta(x, t). \tag{28}$$

From Eq. (23), we have

$$v_0 = u_0 = -1 + z^2 - h^2 + \frac{1}{\beta^2}(1 - y^2). \tag{29}$$

With the help of Eq. (29), Eq. (26) can be written as

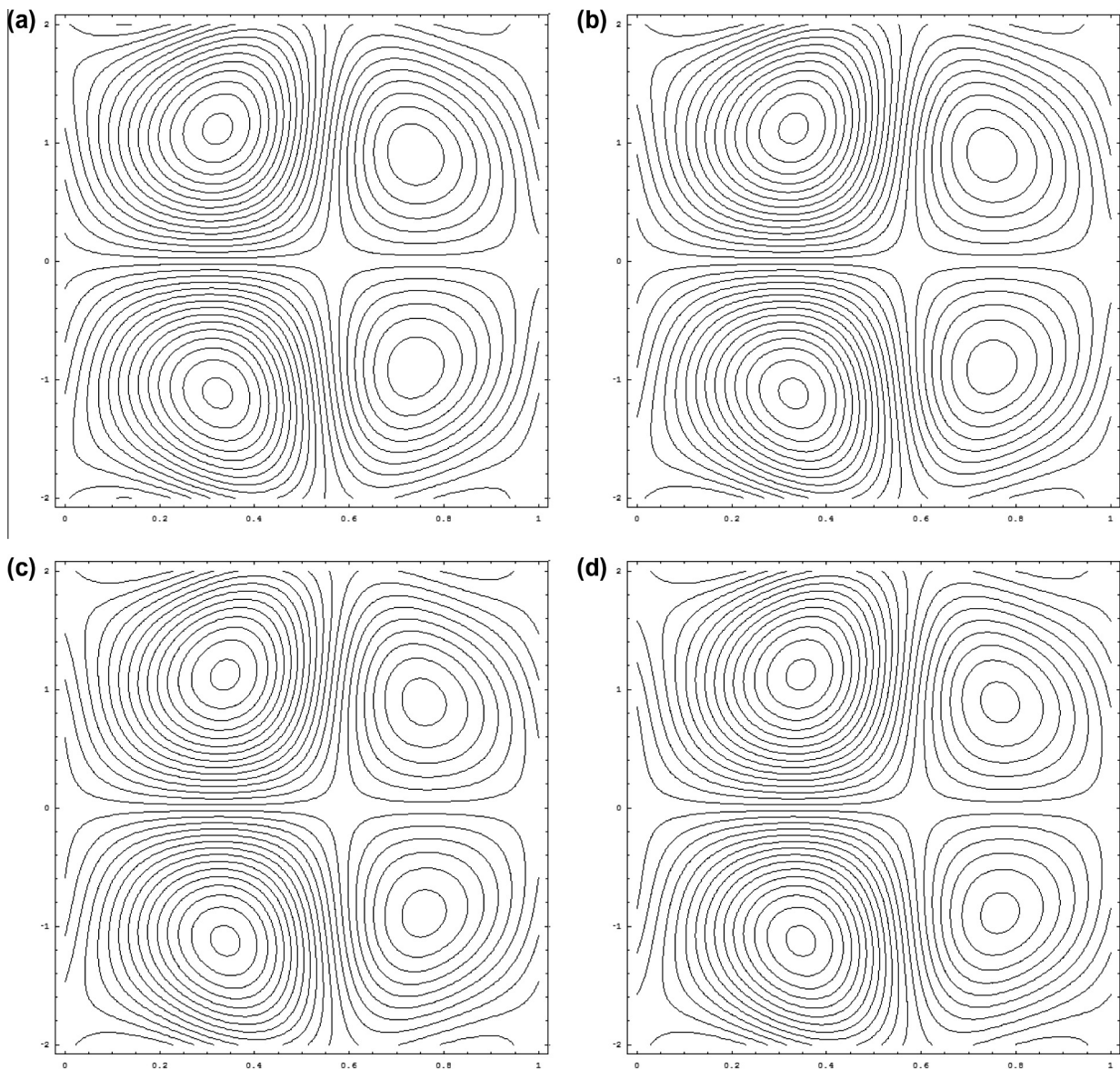


Figure 8 Stream lines for different values of E_2 . (a) For $E_2 = 0.5$, (b) for $E_2 = 0.7$, (c) for $E_2 = 0.9$, (d) for $E_2 = 1.1$. The other parameters are $y = 1$, $\phi = 0.1$, $t = 0.5$, $n = 0.1$, $We = 0.2$, $E_1 = 0.1$, $\beta = 1.5$, $E_3 = 0.01$, $E_4 = 0.2$, $E_5 = 0.3$.

$$\beta^2 \frac{\partial^2 v_1}{\partial y^2} + \frac{\partial^2 v_1}{\partial z^2} = D + \frac{8(n-1)We^2}{\beta^2} y^2 - 8(n-1)We^2 z^2. \quad (30)$$

The solution of the above non-homogeneous linear partial differential equation is calculated as

$$v_1 = \sum_{m=1}^{\infty} \frac{1}{\cosh\left(\frac{\alpha_m}{\beta h}\right)} \left(\frac{2\beta^2 b_{0m} + a_{0m} \lambda_m + \lambda_m b_{0m}}{\lambda_m^2} \right) \times \cosh\left(\frac{\alpha_m}{\beta h} y\right) \cosh\left(\frac{\alpha_m}{h} z\right), \quad (31)$$

where

$$\lambda_m = (\alpha_m/h)^2, \\ \alpha_m = (2m-1)\pi/2, \\ b_{0m} = \frac{2B(-1)^m}{\alpha_m/h},$$

$$B = \frac{8(n-1)We^2}{\beta^2}, \\ C = -8(n-1)We^2, \\ D = 2\pi\phi[2E_2\pi \cos 2\pi(x-t) - (E_5 + 4\pi^2(-E_1 + E_4 + 4E_3\pi^2)) \sin 2\pi(x-t)], \\ a_{0m} = \frac{1}{h} \left(4\pi\phi[2E_2\pi \cos 2\pi(x-t) - (E_5 + 4\pi^2(-E_1 + E_4 + 4E_3\pi^2)) \sin 2\pi(x-t)] \frac{(-1)^m}{\alpha_m/h} + \frac{2Ch^2(-1)^m}{\alpha_m/h} - \frac{4C(-1)^m}{\alpha_m^3/h^3} \right).$$

Finally, the HPM solution upto first iteration leads us to the original solution (when $q \rightarrow 1$)

$$u(x, y, z, t) = v_0 + v_1, \quad (32)$$

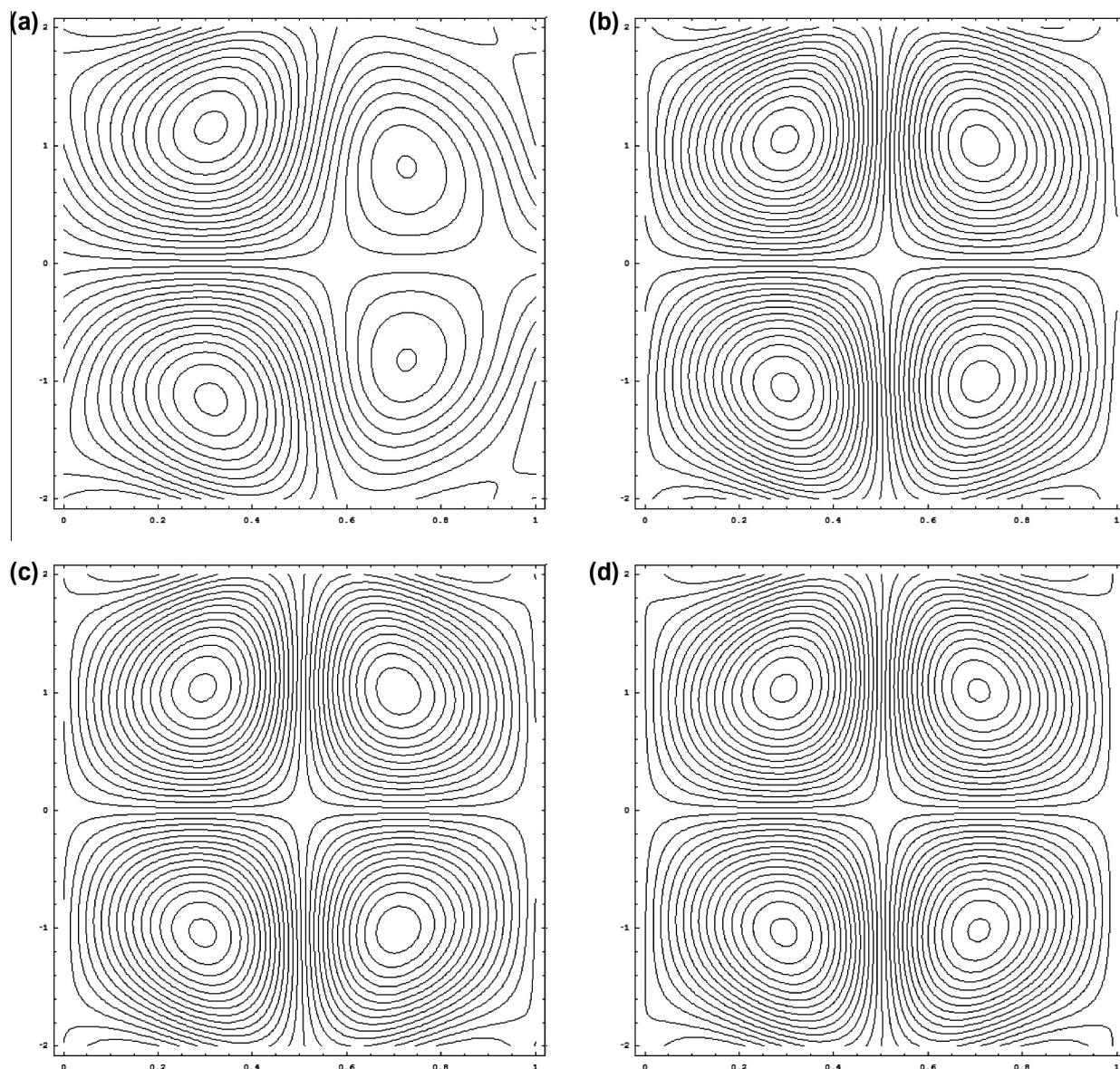


Figure 9 Stream lines for different values of E_3 . (a) For $E_3 = 0.01$, (b) for $E_3 = 0.05$, (c) for $E_3 = 0.09$, (d) for $E_3 = 0.13$. The other parameters are $y = 1$, $\phi = 0.1$, $t = 0.5$, $n = 0.1$, $We = 0.2$, $E_1 = 0.2$, $E_2 = 0.1$, $\beta = 1.5$, $E_4 = 0.1$, $E_5 = 0.3$.

where v_0 and v_1 are defined through Eqs. (29) and (31). By making use of these two equations in the above result, we approach to the following series solution for the velocity distribution

$$\begin{aligned}
 u(x, y, z, t) = & -1 + z^2 - h^2 + \frac{1}{\beta^2}(1 - y^2) \\
 & + \sum_{m=1}^{\infty} \frac{1}{\cosh\left(\frac{\alpha_m}{\beta h}\right)} \left(\frac{2\beta^2 b_{0m} + a_{0m}\lambda_m + \lambda_m b_{0m}}{\lambda_m^2} \right) \\
 & \times \cosh\left(\frac{\alpha_m}{\beta h}y\right) \cos\left(\frac{\alpha_m}{h}z\right). \tag{33}
 \end{aligned}$$

It is observed from the above problem that if we use the limit $\beta \rightarrow 0$, the rectangular duct becomes a two dimensional channel. It is also measured that when $\beta = 1$, the rectangular duct reduces to square duct. Further, it can be noted from the present analysis that if we take Weissenberg number $We = 0$, we return to the viscous fluid problem.

4. Results and discussions

4.1. The uniform velocity distribution

The analytical solutions obtained in above section are discussed graphically in this section. The graphs for velocity profile and stream functions are sketched both for two and three dimensions. Figs. 1–5 are plotted to see the effects of physical parameters namely n, E_1, E_2, E_3 and We on velocity profile. In Figs. 1–3, the velocity profile is plotted against z -coordinate with increasing magnitude of the parameters n, E_1 and E_2 , respectively. It is observed that by increasing the values of all these parameters, the velocity field decreases. However, the variation in the magnitude of velocity is faster when seen for E_1 as compared to n and E_2 . The graphs of the velocity field for different values of E_3 and We are displayed in Figs. 4 and 5, respectively. It is noticed that velocity varies directly with E_3

and We that is if someone increases the magnitude of these given parameters, the velocity curves gets more height and adopt uniform parabolic path throughout the channel. It is also concluded from the results seen in Figs. 1–5 that the maximum velocity is at the center of the channel for small values of all the given parameters. Also the variation of velocity profile remains symmetric and continuous throughout the channel for all the time. The three dimensional analysis of the velocity is also portrayed in (b) parts of the above mentioned figures.

4.2. Trapping scheme

The trapping phenomenon is described by plotting stream lines and is shown through Figs. 6–9. The variation of circulating bolus is presented for pertinent parameters, i.e., We, E_1, E_2 and E_3 . The stream lines for different values of We are sketched in Fig. 6. It is depicted from Fig. 6 that with the increase in the parameter We , the number of trapping bolus decreases on the left side but increases on the opposite side of the channel and size of the bolus is also changing oppositely in both sides of the channel. From Fig. 7, it is evaluated that the more bolus appears with increasing values of the parameter E_1 and the size of bolus is also changing. Figs. 8 and 9 are drawn to show the stream lines for the parameters E_2 and E_3 . It is observed from Fig. 8 that the size of the bolus remains same in left side of the channel but decreases in the other side but the number of bolus does not vary. From Fig. 9, it is noted that the number of bolus increases with the increasing magnitude of E_3 but size of the bolus is changing time by time with E_3 .

5. Concluding remarks

In the present investigation, authors have made attempt to find the analytical solutions for the peristaltic flow of Carreau fluid in a three dimensional rectangular duct having compliant walls. The considered flow is assumed to be incompressible and unsteady and discussed in a three dimensional rectangular coordinate system. The observations are produced under the assumption of long wavelength and low Reynolds number which justifies that the flow is laminar. The obtained governing flow equations are highly non-linear partial differential equations which are solved with the help of well-known series solution technique namely homotopy perturbation method. The effects of all pertinent parameters are included through graphical treatment. From the above mathematical analysis, we have derived that the velocity profile diminishes with the increase in numerical values of n, E_1 and E_2 , while opposite results are observed for E_3 and We . Moreover, the trapping bolus contracts on right side but expands on left side with the variation of We and E_3 . It is also concluded from the above discussion that trapping bolus shows inverse behavior with the change in values of E_1 and E_2 .

Acknowledgment

A. Riaz would like to thank the Higher Education Commission Pakistan for awarding him the Indigenous Scholarship for his Ph.D. studies.

References

- [1] A.H. Shapiro, M.Y. Jaffrin, S.L. Weinberg, Peristaltic pumping with long wavelengths at low Reynolds number, *J. Fluid Mech.* 37 (1969) 799–825.
- [2] T.W. Latham, Fluid Motion in a Peristaltic Pump, M.Sc., Thesis, M.I.T., Cambridge, 1966.
- [3] S. Nadeem, S. Akram, Influence of inclined magnetic field on peristaltic flow of a Williamson fluid model in an inclined symmetric or asymmetric channel, *Math. Comput. Model.* 52 (2010) 107–119.
- [4] S. Nadeem, S. Akram, Heat transfer in a peristaltic flow of MHD fluid with partial slip, *Commun. Nonlinear Sci. Numer. Simul.* 15 (2010) 312–321.
- [5] S. Nadeem, S. Akram, Slip effects on the peristaltic flow of a Jeffrey fluid in an asymmetric channel under the effect of induced magnetic field, *Int. J. Numer. Meth. Fl.* (in press), doi:<http://dx.doi.org/10.1002/fld.2081>.
- [6] S. Nadeem, S. Akram, Peristaltic transport of a hyperbolic tangent fluid model in an asymmetric channel, *Z. Naturforsch.* 64a (2009) 559–567.
- [7] S. Tsangaris, N.W. Vlachakis, Exact solution of the Navier Stokes equations for the fully developed, Pulsating flow in a rectangular duct with constant cross-sectional velocity, *J. Fluid. Eng-T. ASME* 125 (2003) 382–385.
- [8] S. Nadeem, S. Akram, Peristaltic flow of a couple stress fluid under the effect of induced magnetic field in an asymmetric channel, *Arch. Appl. Mech.* 81 (2011) 97–109.
- [9] S. Nadeem, N.S. Akbar, Effects of heat transfer on the peristaltic transport of MHD Newtonian fluid with variable viscosity: application of Adomian decomposition method, *Commun. Nonlin. Sci. Numer. Simul.* 14 (2009) 3844–3855.
- [10] E.F. Elshehawey, N.T. Eladabe, E.M. Elghazy, A. Ebaid, Peristaltic transport in an asymmetric channel through a porous medium, *Appl. Math. Comput.* 182 (2006) 140–150.
- [11] R. Ellahi, A. Riaz, S. Nadeem, M. Ali, Peristaltic flow of Carreau fluid in a rectangular duct through a porous medium, *Math. Prob. Eng.* (2012) 24, <http://dx.doi.org/10.1155/2012/32963>. Article ID 329639.
- [12] S. Nadeem, A. Riaz, R. Ellahi, Peristaltic flow of a Jeffery fluid in a rectangular duct having compliant walls, *Chem. Indust. Chem. Eng. Quart.* 19 (3) (2013) 399–409.
- [13] R. Ellahi, A. Riaz, S. Nadeem, M. Mushtaq, Series solutions of magnetohydrodynamic peristaltic flow of a Jeffrey fluid in eccentric cylinders, *Appl. Math. Inform. Sci.* 7 (4) (2013) 1441–1449.
- [14] R. Ellahi, A. Riaz, S. Nadeem, Three dimensional peristaltic flow of Williamson fluid in a rectangular duct, *Ind. J. Phys.*, doi:<http://dx.doi.org/10.1007/s12648-013-0340-2>.
- [15] M.A. Abd Elnaby, M.H. Haroun, A new model for study the effect of wall properties on peristaltic transport of a viscous fluid, *Commun. Nonlin. Sci. Numer. Simul.* 13 (4) (2008) 752–762.
- [16] K.S. Yeo, B.C. Khoo, W.K. Chong, The linear stability of boundary-layer flow over compliant walls—the effects of the wall mean state, induced by flow loading, *J. Fluids. Struct.* 8 (5) (1994) 529–551.
- [17] N. Takemitsu, Y. Matunobu, Numerical calculation of two-dimensional flow in the channel with a partially compliant wall, *Fluid. Dynam. Res.* 4 (1) (1988) 1–14.
- [18] S. Srinivas, M. Kothandapani, Peristaltic transport in an asymmetric channel with heat transfer, *Int. Commun. Heat. Mass.* 35 (4) (2008) 514–522.
- [19] S. Nadeem, S. Akram, Peristaltic flow of a Jeffrey fluid in a rectangular duct, *Nonlin. Anal.-Real.* 11 (5) (2010) 4238–4247.

-
- [20] S. Maiti, J.C. Misra, Peristaltic flow of a fluid in a porous channel: a study having relevance to flow of bile within ducts in a pathological state, *Int. J. Eng. Sci.* 49 (9) (2011) 950–966.
- [21] C. Davies, P.W. Carpenter, Instabilities in a plane channel flow between compliant walls, *J. Fluid Mech.* 352 (1997) 205–243.
- [22] J.H. He, Homotopy perturbation technique, *Comput. Meth. Appl. Mech. Eng.* 178 (3/4) (1999) 257–262.
- [23] J.H. He, Homotopy perturbation method for solving boundary value problems, *Phys. Lett. A* 350 (1–2) (2006) 87–88.